Supplementary Information

Precise Attolitre Temperature Control of Nanopore Sensors using a Nanoplasmonic Bullseye

Colin R. Crick[†], Pablo Albella[‡], Binghao Ng[‡], Aleksandar P. Ivanov[†], Tyler Roschuk[‡], Michael P. Cecchini[†], Fernando Bresme[†], Stefan A. Maier*[,‡], Joshua B. Edel*[,†]

† Department of Chemistry, Imperial College London, South Kensington Campus, London, SW7 2AZ, United Kingdom

‡ Department of Physics, Imperial College London, South Kensington Campus, London, SW7 2AZ, United Kingdom

* Author to whom correspondence should be addressed.

* Joshua B. Edel – **Address** - Department of Chemistry, Imperial College London, South Kensington Campus, London, SW7 2AZ, United Kingdom. **Email** - joshua.edel@imperial.ac.uk

* Stefan A. Maier - **Address** - Department of Physics, Imperial College London, South Kensington Campus, London, SW7 2AZ, United Kingdom. **Email** - s.maier@imperial.ac.uk

Experimental Details

Device Fabrication Methods

Silicon wafers were used to fabricate the free-standing (100 nm thick) Si_3N_4 membranes using standard photolithography and KOH wet etching as described elsewhere.[34] These membranes are then coated with a 10 nm layer of Chromium and subsequently 100 nm of Gold. The total membrane thickness (including adhesion layer) is 210 nm. Each Si chip has a 5 x 5 mm footprint (300 μm thick). A free-standing SiNx/Au 60 μm x 60 μm membrane was fabricated by removing a patterned area of the Si using KOH wet etching, Figure 1.

Nanopore and Bulls-eye Milling

Nanopore (80 ± 10 nm diameter) and bulls-eye milling was carried out using a focused Ga^+ ion beam (FIB, Zeiss Auriga FEG SEM FIB, acceleration voltage = 20 kV, milling current = 5 pA). The milling times were adjusted to achieve the optimised bullseye geometry (Figure 1). Platinum alignment markers were deposited at the corners of the free standing membrane. This made it for easy location of the freestanding membrane in FIB mode. This was carried out on the same Zeiss Auriga instrument, using SEM exposure in the presence of a gaseous precursor and an acceleration voltage of 20 kV.[10]

Characterisation Techniques

The devices were characterised primarily though scanning electron microscope (SEM) imaging, directly after FIB milling of the structures using the Zeiss Auriga FEG SEM FIB (acceleration voltage = 20 kV). Extinction spectra for the devices were measured with a confocal spectroscopy arrangement using a white light super-continuum laser source (Fianium SC450-4) focused onto the ring side of the structure using a 10X objective (Nikon, NA = 0.30). Transmission through the sample was then collected with a 50X objective (Nikon, NA= 0.45). The sample was scanned using a piezoelectric stage and a 50 μm multimode optical fibre (Thorlabs) was used to spatially define the collection spot. An APD was used to map the structure and spectra were acquired from the centre of the structures using a spectrometer (Princeton) and CCD camera (Princeton PIXIS). The spectra were then normalized to the intensity of the source used to obtain the extinction spectra.

Plasmonic Heating Experiments

The plasmonic heating experiments were carried out on a custom built optical microscope.[10] The complete devices were packaged into a fluidic cell separating the solution filled compartments, each incorporating a non-polarizable Ag/AgCl electrode (Figure 1C). The membranes were mounted in an optical cell with upper and lower electrolyte reservoirs, each filled with aqueous KCl (1 M) and separated by the Au/Si_3N_4 membrane. The pores were heated using a Nd:YAG 532 nm, a HeNe 632.8 nm and a laser diode 685 nm excitation sources. Each source was focused to a diffraction limited spot (Ø ~ 2 μm) at the Au nanopore entrance. In each case the bullseye/nanopore structure was fully illuminated by the Gaussian beam. For each illumination setting, multiple chronoamperometric traces were measured (ranging from −0.3 to 0.3 V with a 0.025 V step and 2.5 s step duration) using an A-M 2400 patch clamp amplifier, with 5 KHz Bessel filter and then sampled at 20 KHz with National Instruments NI USB-6251 DAQ and WinWCP 4.79 acquisition software. From the chronoamperometric traces, I-V plots were extracted with a slope yielding the nanopore conductance. The ionic current was monitored while varying the optical density of the excitation source. A full schematic is shown in Figure 1.

Numerical Heat Calculation Details

In the absence of phase transformations, the temperature distribution around optically stimulated surfaces can be described by the usual heat transfer equation:

$$\rho(r)c(r)\frac{\partial T(r,t)}{\partial t} = \nabla k(r)\nabla T(r,t) + Q_e(r,t) \qquad (1)$$

where r and t are the coordinate and time, T(r,t) is the local temperature, and the material parameters ρ(r), c(r) and k(r) are the mass density, specific heat, and thermal conductivity, respectively. The solution of Equation (1) has a transient state, and after a characteristic time, it reaches its steady state [refs]. Thermal processes in metals are fast, which means that a steady state is rapidly reached for typical incident powers and metal surface dimensions. The function $Q_e(r,t)$ represents an energy (heat) source coming from light dissipation (EM losses) in the materias (see ref. for more details):

In our case, the whole process of light absorption and subsequent heat transfer between the nanostructure and the surrounding medium has been modeled by means of finite element simulations. For easy implementation and reliability of the solution, we have chosen Comsol Multiphysics 4.3a (Comsol Inc., Burlington, MA), which provides state-of-the-art routines to solve partial differential equations (PDEs). In our simulations, we have assumed the EM losses from the EM waves in the NPs as the only heat source. We furthermore and unless otherwise stated, we have assumed that the EM cycle time is short compared to the thermal time scale (adiabatic assumption). In order to take into account heat dissipation in our simulation region, we used a heat flux node across the outer boundaries, defined by the equation:

$$q_0 = h(T_{ext} - T) \qquad (2)$$

where h is the heat transfer coefficient of each medium, dependent on the geometry, material and the ambient flow conditions, T_{ext} is the external temperature (assumed to be the same as the initial temperature of the system), and T is the temperature of the system. The heat transfer coefficient h can often be estimated by dividing the thermal conductivity of the convection fluid by a length scale.

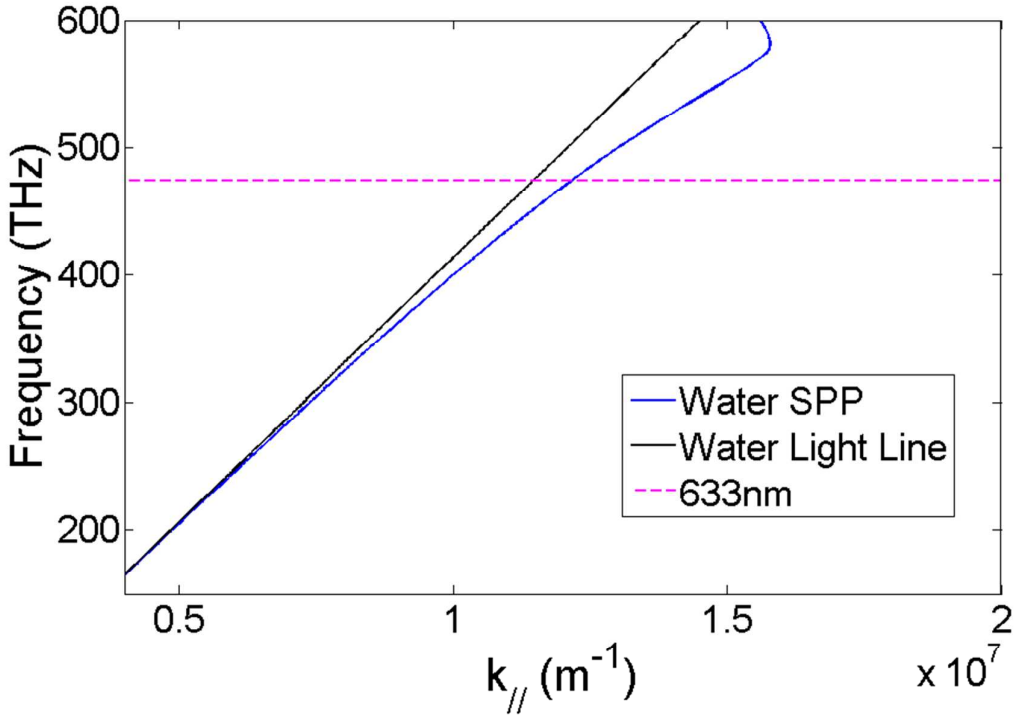

Figure S1. Periodicity vs field enhancement. Please find explanation below.

The SPP dispersion relation on gold-water interface is calculated using Equation (1) and gold permittivity values given by Johnson and Christy. It is given by the blue-solid line in the above figure, where $k_{//} = 2\pi/\lambda_{SPP}$ is the wavevector parallel to the gold-water interface and λ_{SPP} is the wavelength of the SPP. Note that the SPP dispersion relation lies beneath the water light line (black line), which means that light propagating in water cannot be simply coupled into SPPs by illuminating the gold surface with an excitation light source. A coupling mechanism is required to phase match free-space propagating light to the SPPs.

Given an excitation wavelength of 633 nm at normal incidence (indicated by the magenta dotted line), a phase matching of $k_{//} = 1.21 \times 10^7 m^{-1}$ is needed in order for the 633 nm photon to couple to an SPP propagating on a gold-water interface. This is because, at normal incidence, the $k_{//}$ of the free-space photon is zero. The mismatch between the photon and the SPP can be reconciled using a grating structure with a period P, which imparts a parallel wavevector equivalent to $2\pi/P$ to the photon. This implies that, in the case of a bullseye structure consisting of a series of concentric rings, a ring periodicity of 518nm is needed to phase-match the 633 nm excitation light to the SPP [ref 1 (below)]. This is our starting point for designing a bullseye nanopore that allows plasmons to be excited and propagated towards the nanopore itself.

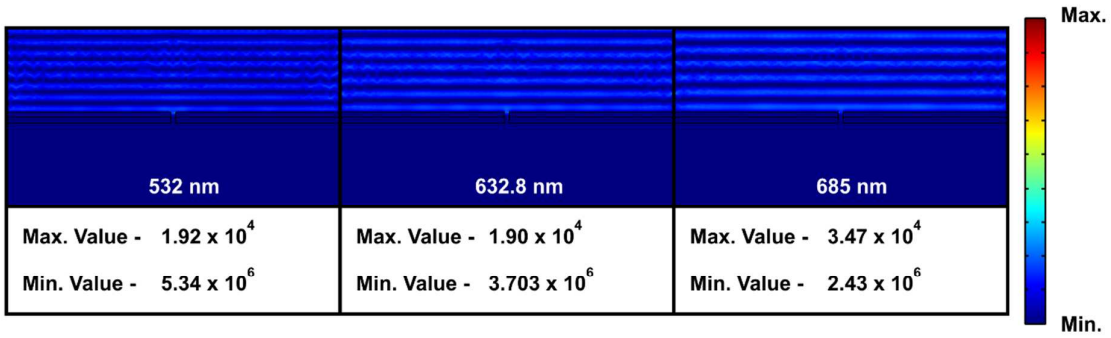

Figure S2. Side-view of field distribution at 532, 632.8 and 685 nm for the 518 nm bullseye periodicity.

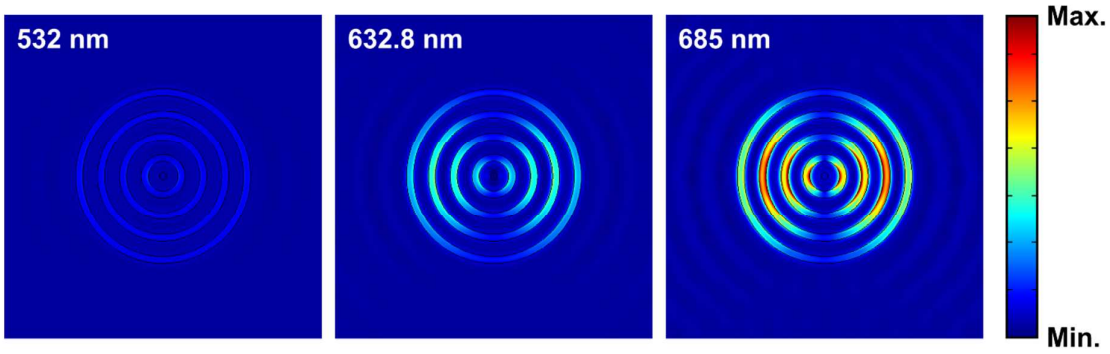

Figure S3. Top-view of field distribution at 532, 632.8 and 685 nm for the 250 nm bullseye periodicity.

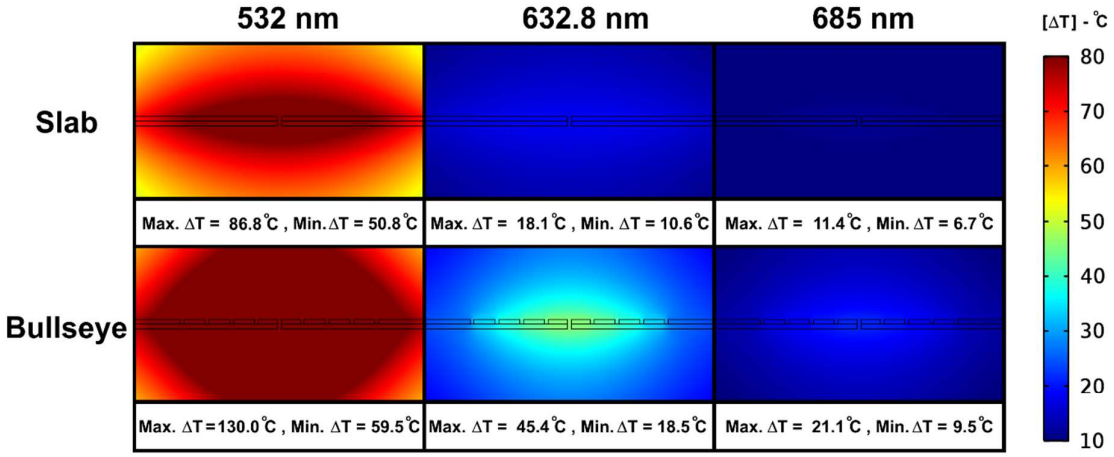

Figure S4. Shows simulated temperature maps for both slab and bullseye conditions at the various laser wavelengths.

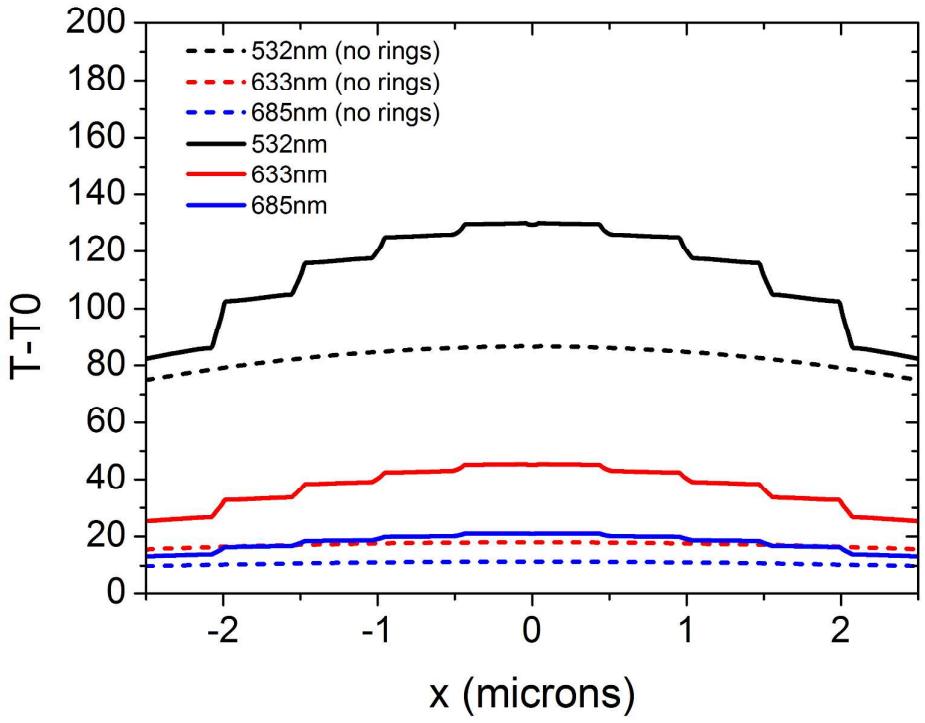

Figure S5. Modelled one-dimensional temperature plot, shows the temperature change (°C) for along at the top of gold surface transecting the nanopore. The heating is given for each laser for both bullseye and no ringed cases. The simulated laser power was 5 mW. The nanopore is situated at x = 0 μm.

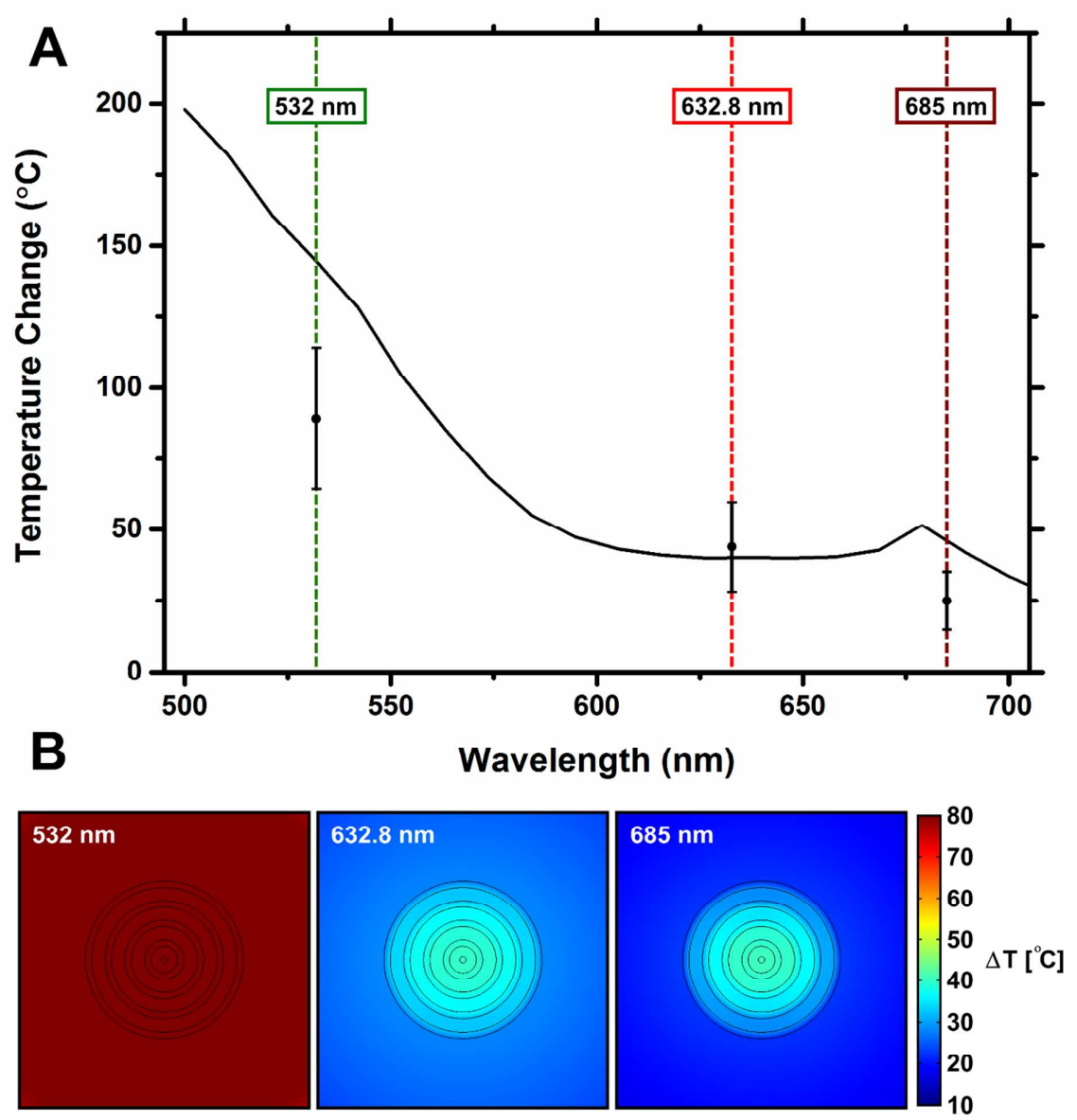

Figure S6. Temperature data for a bullseye with 250 nm period. (A) Modelled temperatures are shown with a solid black line and are values for a modelled 5 mW of laser power, the experimental results are plotted for each laser used at a power of 5 mW. (B) Modelled temperature map images for each laser at 5 mW of simulated power.

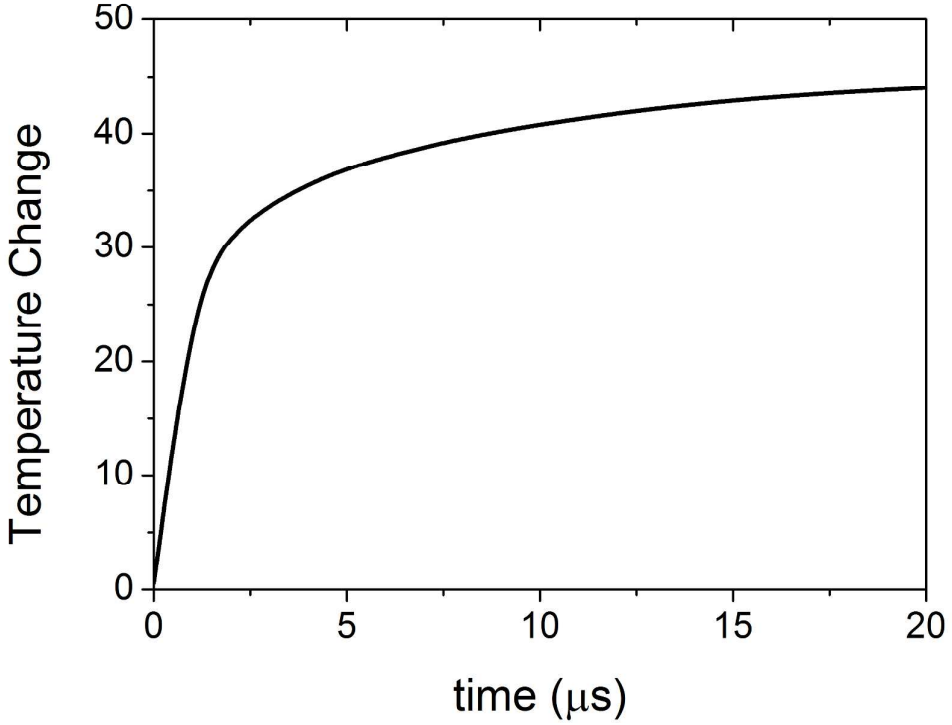

Figure S7. Temperature change with time of irradiation. The modelled data is based on a simulated bullseye nanopore, irradiated with the 632 nm laser at 5 mW of power.

References:

1) Maier, S. A., *Plasmonics: Fundamentals and Applications*. Springer US: 2010.